
Tidal Disruption Event:
Star torn apart from neighboured black hole

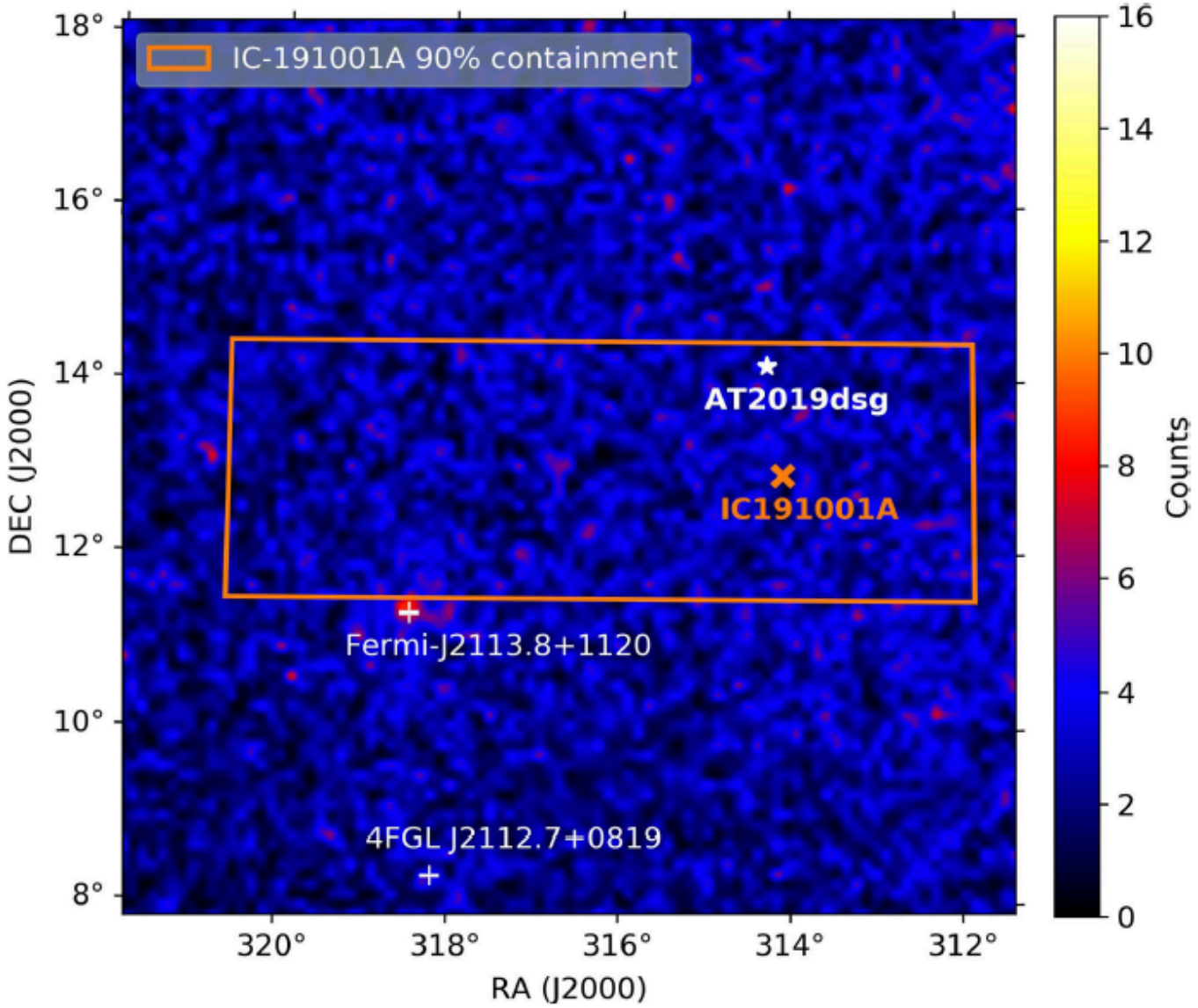

Extended Data Fig. 6 | LAT count map of the Region Of Interest (ROI). The map shows the integrated search period G3, showing the IC191001A 90% localisation region in orange. The position of AT2019dsg is marked by a white star. The neutrino best-fit position is marked with a orange '×'. Two gamma-ray sources are significantly detected ($\geq 5\,\sigma$) in the ROI but outside the neutrino uncertainty region as marked with white crosses. There is no excess consistent with the position of AT2019dsg.

Authors: Zwicky Transient Facility observers, NOT IceCube collaboration

Coming from TDE ?

1 October 2019 IC191001A ~200 TeV neutrino, 56% signalness, 26deg^2

GCN: *Given that the track is partially obscured by a natural dust layer in the ice, the 90% uncertainty region reported by the reconstruction algorithms is larger than average error contours. There are two Fermi 4FGL catalogue sources within the 90% contour. The nearest is 4FGL J2052.7+1218, located 1.1 degrees away at the edge of the 50% localization region. One additional source, 4FGL J2115.2+1218, is also located within the 90% contour at a distance of 4.8 degrees from the best fit.*

=> ZTF discovered TDE 9 April 2019

30 May 2020 IC 200530A, ~80 TeV neutrino, 59% signalness, 25deg^2

GCN: *There are two Fermi 4FGL catalogue sources within the 90% contour, both lying close to the best fit position. The nearest is 4FGL J1702.2+2642, located 0.20 degrees from the best fit position. The other, 4FGL J1659.0+2627, is located 0.56 degrees from the best fit.*

=> ZTF discovered TDE 27 April 2019, but only later classified as TDE

Why considered interesting?

TDE density on the sky: <= 2 radio-emitting TDEs in the sky at any given time

=> Finding one TDE in 80deg^2 of neutrino-followup => 0.5% chance
Considering high bolometric luminosity => 0.2% chance

Classified as TDE based on optical spectrum

- optical/UV continuum well-described as black-body

- Peak luminosity in top 10% of known 40 optical TDEs

- Black hole mass estimated ~3 10^7 $M_\odot$

- X-ray consistent with thermal emission from black body *(radius <Schwarzschild radius?)*
  Exponential decrease of X-ray flux could mean cooling or X-ray obscuration

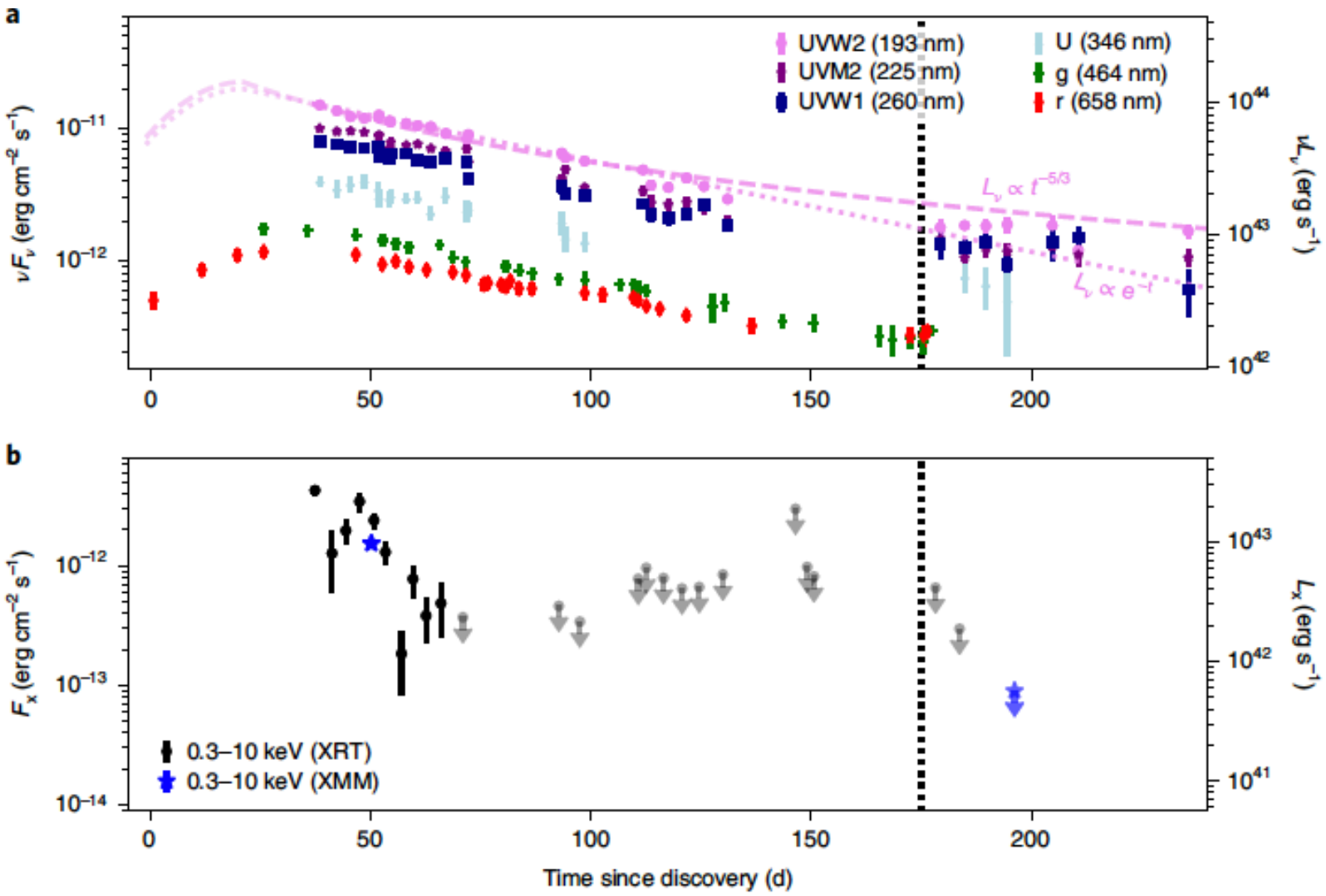

UV (top)
and
X-ray (bottom)

Fig. 1 | Multiwavelength lightcurve of AT2019dsg. a, The optical photometry in bands g and r from ZTF (in green and red, respectively), alongside UV observations in bands UVW2, UVM2, UVW1 and U from the Neil Gehrels Swift Observatory (Swift)-UVOT (Ultraviolet/Optical Telescope) (in pink, violet, navy and blue, respectively). The left axis shows νF_ν, where F_ν is the spectral flux density at frequency ν, while the right axis shows νL_ν, where L_ν is the luminosity at frequency ν. The late-time UV observations show an apparent plateau, which is not captured by a single-power-law decay. The dashed pink line illustrates a canonical $t^{-5/3}$ power law, while the dotted pink line illustrates an exponentially decaying lightcurve. Neither model describes the UV data well. **b**, The integrated X-ray energy flux, from observations with Swift-XRT (X-Ray Telescope) and XMM-Newton, in the energy range 0.3–10 keV. Arrows indicate 3σ upper limits. The vertical dotted line illustrates the arrival of IC191001A. Error bars represent 1σ intervals.

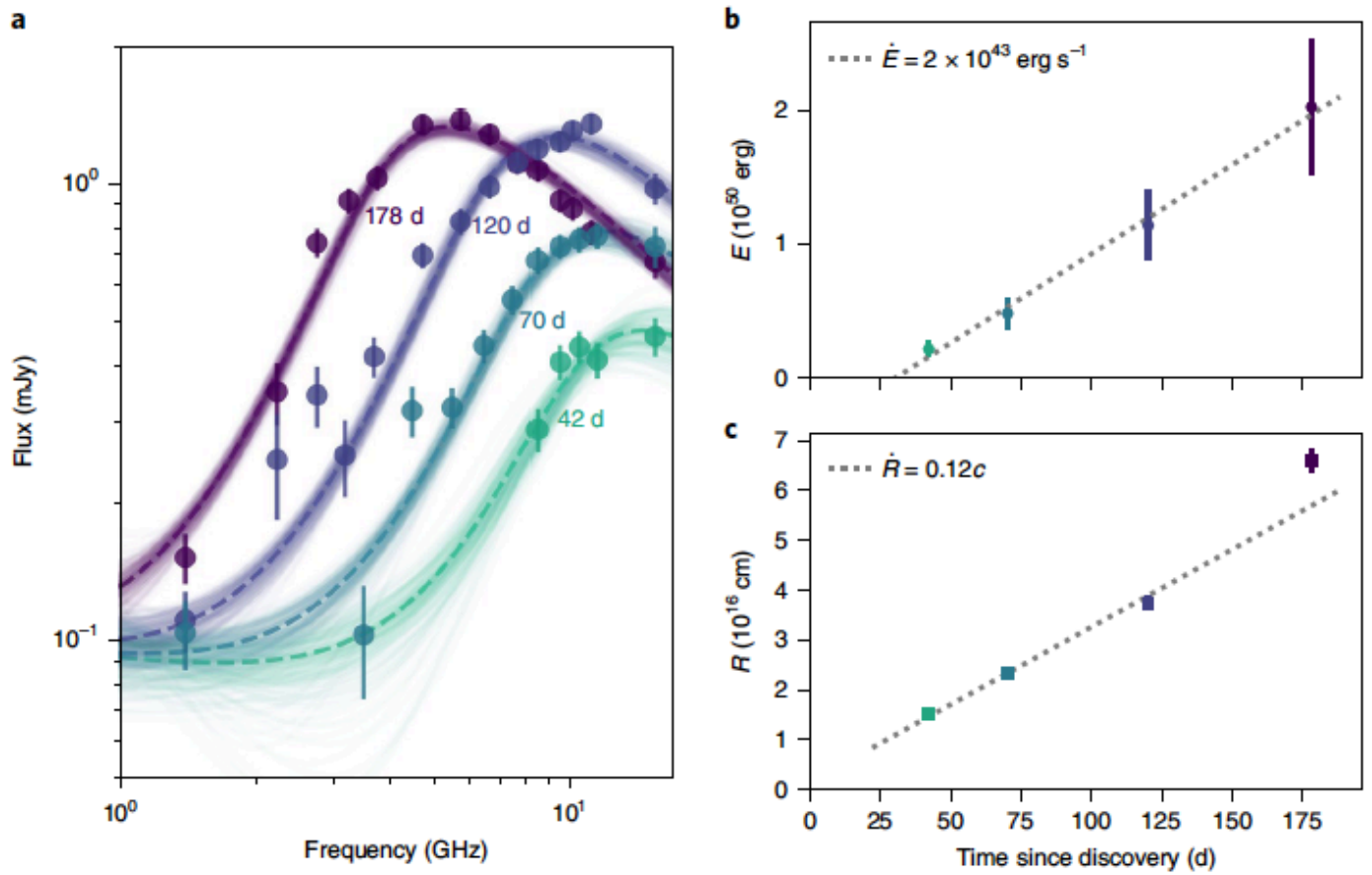

Radio (GHz) observations indicating non-thermal synchrotron radiation
⇒ Electron acceleration

Linear increase of energy
-> constant energy injection

Fig. 2 | Synchrotron analysis of AT2019dsg. a, Radio measurements from MeerKAT (1.3 GHz), the Karl G. Jansky Very Large Array (VLA; 2–12 GHz) and the Arcminute Microkelvin Imager (AMI; 15.5 GHz) at four epochs with times listed relative to the first optical detection. The coloured lines show samples from the posterior distribution of synchrotron spectra fitted to the measurements at each epoch, and the dashed lines trace the best-fit parameters for that epoch. The free parameters are the electron power-law index ($p = 2.9 \pm 0.1$) and the host baseline flux density, plus the magnetic field and radius for each epoch. **b**, The energy at each epoch for a conical outflow geometry with an half-opening angle of 30°. The dotted line indicates a linear increase of energy. **c**, The corresponding radius for each epoch, with a dotted line illustrating a linear increase. Error bars represent 1σ intervals.

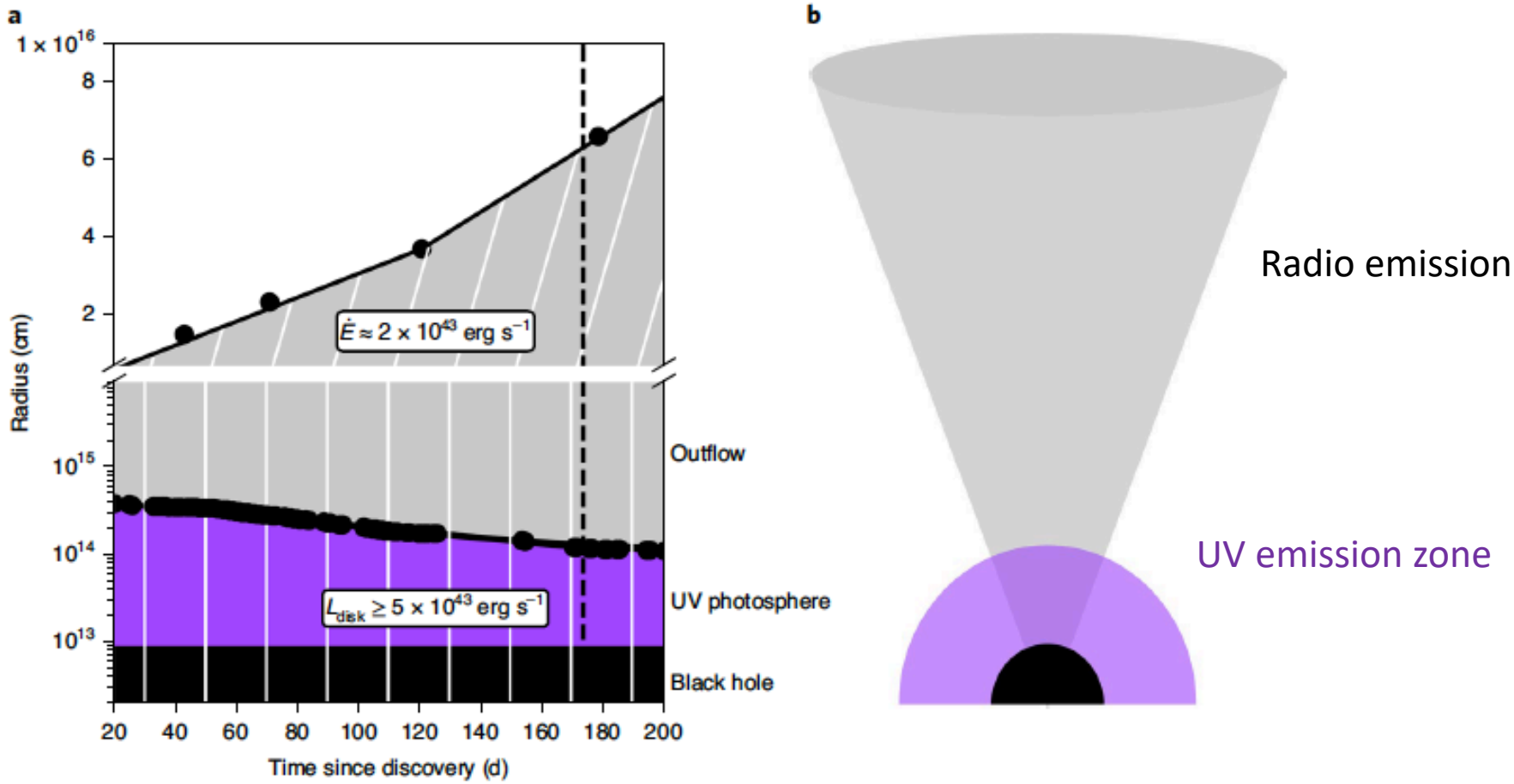

Fig. 3 | Diagram of the three emission zones in AT2019dsg. a, The temporal evolution of the three emission regions. **b**, The geometry of these same regions. The size of the region responsible for radio emission (in grey), as well as the blackbody radius for the UV emission (in purple), is derived from data. The Schwarzschild radius is plotted in black for a black hole mass of $3 \times 10^7 M_\odot$. The white lines in **a** represent a continuous outflow with velocity *c*.

Checks of plausibility of neutrino production at the site

- 3 distinct emission zones established,

- Hillas criterium fullfilled: Assuming neutrino with 0.05E of parent proton energies and magnetic fields from synchrotron estimates -> 160PeV allowed

- Target photons or protons:
  For UV photons: ~0.8PeV, for X-ray ~0.05PeV -> both compatible
  Protons require high density: from unbound stellar debris? From pre-existing gas?

alerts. Approximating the sharply peaked $p\gamma$ neutrino spectrum as a monoenergetic flux anywhere in the range $0.2\,\mathrm{PeV} \lesssim \epsilon_\nu \lesssim 1\,\mathrm{PeV}$, we find $N_\nu = (E_{\nu,\mathrm{tot}}/\epsilon_\nu)(A_{\mathrm{eff}}/4\pi D_{\mathrm{L}}{}^2) \approx 0.03$. Thus any optically thick $p\gamma$ scenario would be sufficient to produce the neutrino under these assumptions.

In contrast to a peaked $p\gamma$ neutrino spectrum, for pp production the neutrinos would instead follow a power law. Many of these neutrinos would then fall below the threshold of IceCube's alert selection. The associated gamma rays would however fall within

← Proton-photon plausible

← Proton-proton
not necessarily > alert threshold

IceCube has already searched for correlations between a sample of TDEs and a neutrino dataset dominated by lower-energy events, and reported that thermal TDEs account for less than 39% of the diffuse astrophysical flux under the assumption of standard candles following a power-law spectrum3

But:
- The cited ICRC proceeding lists 26% (?) at 90%CL
- The cited analysis was focussing on time periods <100days after peak

Conclusion/outlook:

target. Neutrinos can uniquely serve as probes of the inner region of TDEs, using this novel method of extragalactic neutrino tomography. Now that a persistent central engine has been revealed in coincidence with a high-energy neutrino, we can begin to shed light on the role of TDEs as astrophysical accelerators.

ANTARES analysis

Data sample: TDE start – February 2020

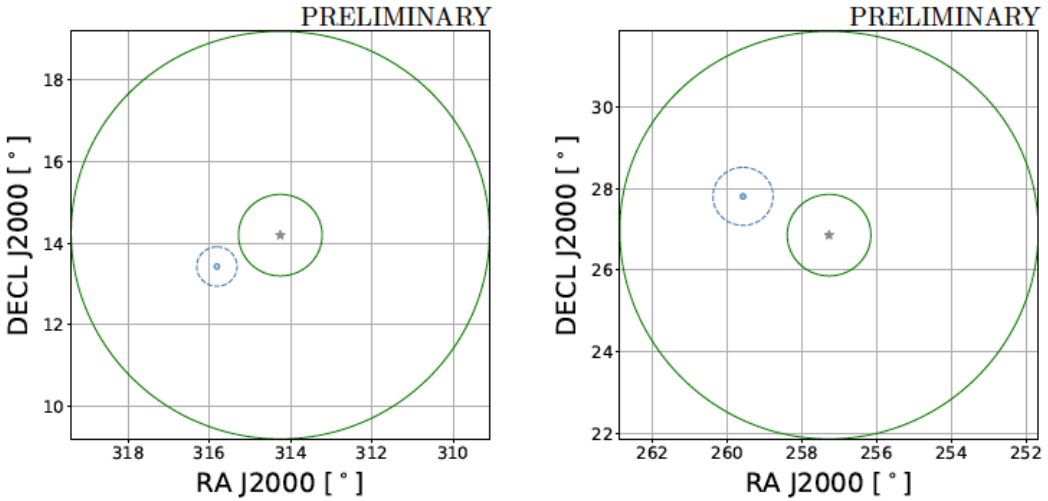

Source	topology	(RA, δ) deg	$\Delta\Psi$ deg	MJD	date dd/mm/year	f
AT2019dsg	track	(315.8, 13.4)	1.7	58890.99	11/02/2020	0.35
AT2019fdr	track	(259.6, 27.8)	2.3	58751.08	25/09/2019	0.15

Table 2: Results of the search at the location of AT2019dsg and AT2019fdr in terms of best-fit number of signal events $\hat{\mu}_{\rm sig}$, p-value, 90% C.L. sensitivity and upper limits on the one-flavour neutrino flux normalisation $\Phi_0^{90\%\rm C.L.}$ (in units of $\rm GeV^{-1}cm^{-2}s^{-1}$), and on the one-flavour neutrino fluence $\mathcal{F}^{90\%\rm C.L.}$ (in units of $\rm GeVcm^{-2}$), for different values of the spectral index γ. The boundaries, $E_{\rm min}$ and $E_{\rm max}$, of the energy range containing 90% of the expected signal events, employed in the calculation of the fluence, are listed in the last column.

Source		Results						
Name	γ	$\hat{\mu}_{\rm sig}$	p-value	$\Phi_0^{90\%\rm C.L.}$		$\mathcal{F}^{90\%\rm C.L.}$		$\log(\frac{E_{\rm min}}{\rm GeV})$ - $\log(\frac{E_{\rm max}}{\rm GeV})$
				sensitivity	limit	sensitivity	limit	
AT2019dsg	2.0	< 0.1	12%	7.3×10^{-8}	1.0×10^{-7}	14	19	3.6 - 6.6
	2.5	0.2	10%	1.5×10^{-5}	2.2×10^{-5}	29	43	2.8 - 5.5
	3.0	0.7	8.9%	1.2×10^{-3}	2.0×10^{-3}	230	380	2.1 - 4.7
AT2019fdr	2.0	0.5	6.7%	8.5×10^{-8}	1.3×10^{-7}	15	23	3.6 - 6.6
	2.5	0.5	7.9%	2.1×10^{-5}	3.0×10^{-5}	39	55	2.8 - 5.5
	3.0	0.6	9.1%	2.0×10^{-3}	3.0×10^{-3}	360	540	2.1 - 4.7